Microvascular Research 152 (2024) 104648

Contents lists available at ScienceDirect

Microvascular Research

journal homepage: www.elsevier.com/locate/ymvre

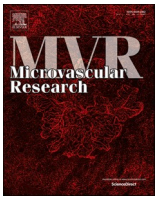

Absolute retinal blood flow in healthy eyes and in eyes with retinal vein occlusion

Thibaud Mautuit [a,b], Pierre Cunnac [a,b], Frédéric Truffer [c], André Anjos [d], Rebecca Dufrane [a,b], Gilbert Maître [c], Martial Geiser [c], Christophe Chiquet [a,b,*]

[a] Department of Ophthalmology, University Hospital of Grenoble-Alpes, France
[b] Grenoble-Alpes University, HP2 Laboratory, INSERM U1042, Grenoble, France
[c] System Engineering Institute, HES-SO, Sion, Switzerland
[d] Idiap Research Institute, Martigny, Switzerland

ARTICLE INFO

Keywords:
Retinal blood flow
Ocular blood flow
Healthy
Retinal vein occlusion
Adaptive optics
Doppler velocimetry

ABSTRACT

Purpose: To measure non-invasively retinal venous blood flow (RBF) in healthy subjects and patients with retinal venous occlusion (RVO).

Methods: The prototype named AO-LDV (Adaptive Optics Laser Doppler Velocimeter), which combines a new absolute laser Doppler velocimeter with an adaptive optics fundus camera (rtx1, Imagine Eyes®, Orsay, France), was studied for the measurement of absolute RBF as a function of retinal vessel diameters and simultaneous measurement of red blood cell velocity. RBF was measured in healthy subjects (n = 15) and patients with retinal venous occlusion (RVO, n = 6). We also evaluated two softwares for the measurement of retinal vessel diameters: software 1 (automatic vessel detection, profile analysis) and software 2 (based on the use of deep neural networks for semantic segmentation of vessels, using a M2u-Net architecture).

Results: Software 2 provided a higher rate of automatic retinal vessel measurement (99.5 % of 12,320 AO images) than software 1 (64.9 %) and wider measurements (75.5 ± 15.7 μm vs 70.9 ± 19.8 μm, $p < 0.001$). For healthy subjects (n = 15), all the retinal veins in one eye were measured to obtain the total RBF. In healthy subjects, the total RBF was 37.8 ± 6.8 μl/min. There was a significant linear correlation between retinal vessel diameter and maximal velocity (slope = 0.1016; $p < 0.001$; $r^2 = 0.8597$) and a significant power curve correlation between retinal vessel diameter and blood flow ($3.63 \times 10^{-5} \times D^{2.54}$; $p < 0.001$; $r^2 = 0.7287$). No significant relationship was found between total RBF and systolic and diastolic blood pressure, ocular perfusion pressure, heart rate, or hematocrit. For RVO patients (n = 6), a significant decrease in RBF was noted in occluded veins (3.51 ± 2.25 μl/min) compared with the contralateral healthy eye (11.07 ± 4.53 μl/min). For occluded vessels, the slope between diameter and velocity was 0.0195 ($p < 0.001$; $r^2 = 0.6068$) and the relation between diameter and flow was $Q = 9.91 \times 10^{-6} \times D^{2.41}$ ($p < 0.01$; $r^2 = 0.2526$).

Conclusion: This AO-LDV prototype offers new opportunity to study RBF in humans and to evaluate treatment in retinal vein diseases.

1. Introduction

Abnormal variations in retinal blood flow (RBF) have been reported in a variety of ocular diseases, including age-related macular degeneration (Burgansky-Eliash et al., 2014; Ehrlich et al., 2009; Pemp and Schmetterer, 2008), glaucoma (Sehi et al., 2014), and retinal vein occlusion (RVO) (Arsene et al., 2002; Chen et al., 1998; Pournaras et al., 2008; Tranquart et al., 1998), as well as in systemic diseases such as diabetes (Grunwald et al., 1992; Pournaras and Riva, 2013) or systemic hypertension (Gutfreund et al., 2013; Lim et al., 2013; Ritt et al., 2012). Measurement of RBF is essential for understanding the pathophysiology of ocular and systemic diseases and is also key to the evaluation of therapeutic strategies (Pemp et al., 2010).

RBF depends on the vascular diameter and velocity of red blood cells. Several techniques have been developed for estimating RBF in the human eye, such as fluorescein angiography (Rechtman et al., 2003),

* Corresponding author at: University Ophthalmology Clinic, University Hospital of Grenoble Alpes, Grenoble Alpes University, 38043 Grenoble cedex 09, France.
E-mail address: cchiquet@chu-grenoble.fr (C. Chiquet).

https://doi.org/10.1016/j.mvr.2023.104648
Received 10 August 2023; Received in revised form 30 November 2023; Accepted 13 December 2023
Available online 18 December 2023

Doppler optical coherence tomography (OCT) (Doblhoff-Dier et al., 2014; Leitgeb et al., 2014; Werkmeister et al., 2012), laser blood flowmetry (Garcia et al., 2002; Guan et al., 2003; Yoshida et al., 2003), laser Doppler velocimetry (LDV) (Garhofer et al., 2012; Riva et al., 1972; Riva et al., 1985) and more recently laser Doppler holography (Puyo et al., 2020). Each device has its proper limitations and some devices allow measurement simultaneously in different vessels whereas others allow measurement of one specific vessel. Current limitations of previous LDV devices include the lower resolution of the fundus camera for the measurement of inner retinal diameter and the inability to perform simultaneous measurements of velocity and vessel diameters. The Canon Laser Doppler (Garcia et al., 2002) allowed simultaneous measurements of retinal vessel diameter and blood flow but is not available at this time and thus no LDV device is commercially available.

Recent and innovative technology using adaptive optics (AO) aims to correct low-order and high-order ocular aberrations, enhance performance of the optical systems, and allows for high-resolution imaging of retinal vessels. For instance, the AO Instrument rtx1 provides in vivo retinal images with high lateral resolution (1.6 μm per pixel) and a quantitative analysis of microvascular structures, especially measurement of retinal arteriolar wall thickness (Koch et al., 2014). The resolution of the AO images is about 3-fold higher than with images acquired by standard retinograph (with a resolution of 4147 × 2764 pixels). Moreover, the image of the AO is coded at 16 bit whereas the standard retinograph are coded only at 8 bit.

In order to counterbalance the limitations of present technologies, we developed an approach based on simultaneous measurements of retinal vessel diameters using AO technology and blood velocities with bidirectional LDV. The aim of the study was to report the results of experiments investigating the validity of blood flow measured by this new prototype AO-LDV in healthy subjects and patients with retinal venous occlusion (RVO).

2. Methods

2.1. AO-LDV device

The laser Doppler velocimeter (Patent: FR1560450) was combined with an adaptive fundus camera (rtx1, Imagine Eyes®) by introducing a beam-splitter into the illumination path close to a pupil's image. Technical details were provided in a recent publication (Truffer et al., 2020). In practice, rtx1 provides a 4° × 4° fundus area (i.e., approximately 1.2 × 1.2 mm in emmetropic eyes) illuminated at 840 nm by a temporally low coherent light emitting diode flashed flood source, and a stack of 40 fundus images is acquired in 4 s (10 images/s) by a charge-coupled device camera. Each fundus image is matched to a spectrum pair provided by LDV, measured at 830 nm. The probing beam and two scattered beams, selected at the pupil plane, lie in the same plane. To bring the velocity vector (i.e., the vessel) into this plane, a Dove prism rotates that plane along the optical axis. This adjustment is done with the use of a diffraction grating producing a sheet of light in the same plane which produces a line on the retina, so that it can be visually aligned with the vessel on the screen of the rtx1. The two scattered beams are collected by two avalanche photodiodes which deliver two beating signals between the light backscattered by the tissue and by the moving red blood cell which Doppler effect shifts the light. The angle between the two scattered beams, defined by the optical system, and the two Doppler signals from the detectors, allow an absolute calculation of the velocity of the red blood cells. This assumes that all red blood cells are moving in the same direction and that the flow is laminar, which determine the velocity distribution (constant up to a maximum velocity then zero) and thus the Doppler shifts distribution.

The initial prototype previously described (Truffer et al., 2020) underwent two significant improvements: (i) development of an external fixator allowing for the measurement of temporal and nasal retinal vessels of both eyes and replacing the internal target of the rtx1 designed for macular acquisition, and (ii) avoiding the parallax problem. Due to the fact that LDV uses the illumination path and not the optical imaging part with adaptive correction, the focal plane of the illumination path is not well defined. To solve this parallax problem, we introduced lasers in the detections paths which illuminate the fundus point of detection. By adjusting the direction of propagation of both lasers, we ensure that the light paths of probing and detections are crossing on the vessel.

2.2. Study design and subjects

The study was conducted in accordance with the Declaration of Helsinki for research involving human subjects and adhered to Good Clinical Practice guidelines. Written informed consent (required for the ethics committee) was obtained from subjects after explanation of the study. This study was approved by the local institutional review board (IRB #6705, CCP Grenoble, France) before the study began.

The following inclusion criteria were applied for all subjects: affiliation to the French national health insurance system, age between 18 and 80 years, and good ocular fixation. RVO patients were included if they had central or branch RVO assessed by fluorescein angiography and OCT. Exclusion criteria were: (a) for all subjects: ametropia ≥3 diopters spherical equivalent, on-going treatment using drugs with a potential effect on intraocular pressure, tropicamide hypersensitivity, lack of compliance, any history of ocular inflammation, aphakia, ocular trauma, optic neuropathy, retinopathy, and/or severe dry eye; (b) for healthy subjects: presence of ocular or general disease, use of any medication; (c) for RVO patients: anti-vascular endothelial growth factor or dexamethasone implant intravitreal injection within the 4 months before the study.

All participants underwent a detailed medical history-taking and complete examination, including best corrected visual acuity, air pulsed tonometry, slit lamp biomicroscopy, indirect fundoscopy, fundus photography (CR-2 CANON fundus camera; Canon™ Europa, Amstelveen, The Netherlands), and axial length measurement (Zeiss IOL Master®, Carl Zeiss Meditec, Jena, Germany). Central subfield is defined as the circular area 1 mm in diameter centered around the center point of the fovea and has been measured using SD-OCT (Heidelberg Spectralis HRA + OCT, Heidelberg Engineering, Heidelberg, Germany).

A blood count for hematocrit was performed within 30 days prior to the examination. Examinations were performed after pupil dilation using 1 % topical tropicamide (Théa, Clermont-Ferrand, France).

Blood pressure and heart rate values were obtained before ocular measurements Healthy subjects and RVO patients were recruited during the same period, and RBF measurements were recorded according the same procedure. RBF measurement was performed after 15 min of rest. One major difficult task was to obtain an excellent fixation of the eye for a correct positioning of the probe on the retinal vein and thereafter keeping this position during the measurement. The rtx1's internal fixation point does not allow the probe to be positioned on the temporal and nasal retinal veins. Therefore, we added an external fixation point for the contralateral eye, which is made up of one small screen that the subject's contralateral eye views through an ocular (Supplemental data). A microprocessor-generated cross on the screen is moved with a joystick by the operator in order to reach temporal and nasal veins with the probing beam. Obtaining a good fixation was obviously more difficult in RVO patients.

Each retinal vessel was systematically measured three consecutive times. As illustrated in Fig. 1, RBF was measured on the main retinal veins, before the first bifurcation or on the two daughter retinal vessels if the bifurcation was too close to the optic disc. For healthy subjects, bifurcations were studied whenever possible depending on the vascular tree of the individual.

In RVO patients, measurements were done on the main inferior and superior temporal retinal veins in the cases of CRVO, and the main superior temporal retinal vein in the case of superior BRVO. Aflibercept (Bayer, Leverkusen, Germany) intravitreal injections were performed at

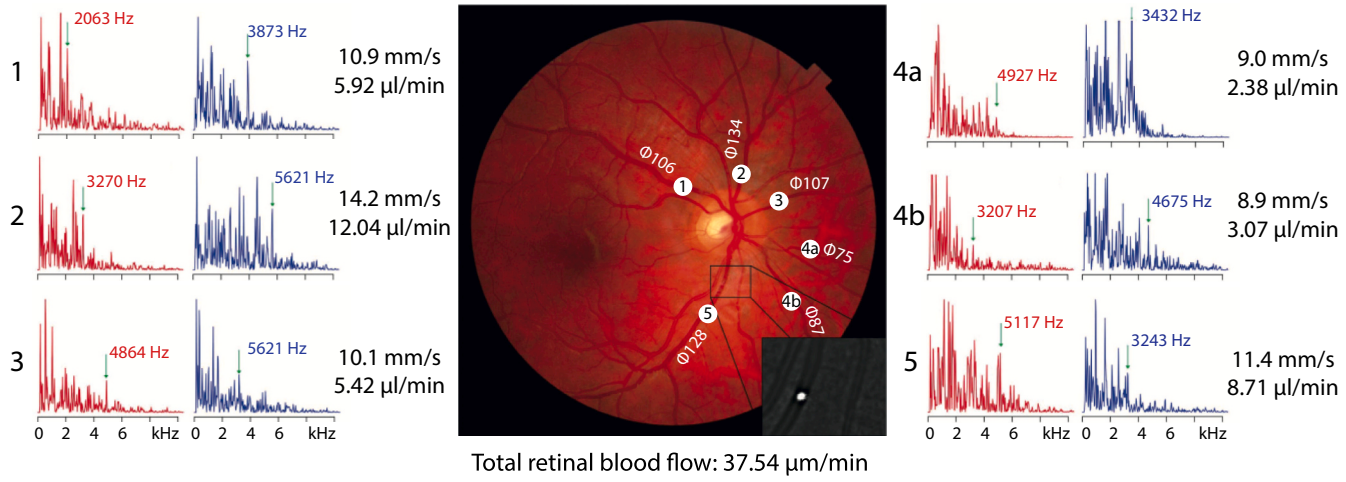

Fig. 1. Total retinal blood flow in one healthy subject.
Each vein emerging from the optic disc was measured. The AO image, used to obtain the vein diameter of each vein and the corresponding diameter is represented on the fundus photograph. Velocity [mm/s] is obtained using the couple of spectra from which the flow is derived [µl/mm]. The total retinal blood flow RBF for this eye is 37.54 µl/min. Note that retinal veins 4a and 4b are first daughter veins whereas the other veins are mother veins. The small figure in black and white illustrates the white spot being the probing laser, centered within the retinal vein.

a dose of 2 mg for RVO patients when required during the follow-up after inclusion in the study, and RBF measurement was repeated 1 month after each injection.

2.3. Data analysis

2.3.1. Vessel diameter

Retinal vessel diameters were measured using software 1 for the evaluation of RBF and these measurements were considered as the standard reference in this study. Software 2 based on the use of deep neural networks for semantic segmentation was developed to improve vessel identification in AO images and was evaluated in a series of measurements in this study. Software 2 was not used for RBF measurement in this study.

The conversion from n pixels to physical distance d is based on the publication of Bennet (Bennett et al., 1994) and was provided by Imagine Eyes©: 19.269 *(L − 1.82) / 373.87 where L is the axial length in millimeters of the eye under examination. The pixel to micron factor is estimated to 1.14 for a normal eye (axial length of 24 mm).

2.3.1.1. Software 1. The diameter of a particular vessel was measured in the image as the width in pixels of this darker path. Several profiles perpendicular to the vessel axis were analyzed and the vessel edges detected in each profile as the two transitions light-to-dark and dark-to-light along the profile. The profile analysis to detect vessel edges was already developed in a previous work (Truffer et al., 2020). However, the method of combining the profiles was different here. In the previous work, a mean profile was computed from all the profiles and edge detection was applied on the mean profile. Here, the profiles were analyzed independently and the vessel diameter was determined as the mean of the edge distances measured in each profile by applying robust statistics, i.e., statistics discarding outliers.

However, the major improvement is the introduction of an automatic vessel detection method. The method assumes that the vessel is darker than the background, is more or less straight and is behind or very close to the spot created by the probing beam on the retinal surface. First, the beam spot was simply detected as the set of pixels surrounding the pixels of maximal intensity. Then, the vessel was detected by cross-correlation with a synthetic pattern representing a straight vessel of mean width. A total of 12 vessel orientations (every 15°) were checked and the pattern translation was allowed at a resolution of one pixel up to a maximal distance with respect to the beam spot center. The vessel position and orientation were those corresponding to the maximal cross-correlation value. The software returned the mean diameter and its corresponding standard deviation as well as the distance between the probing beam and the vessel. In the case that the standard deviation of the diameter is above 10 %, no values are returned.

2.3.1.2. Software 2. Another approach to automatic analysis based on the use of deep neural networks for semantic segmentation of vessels and the laser spot reflection on the infrared image was evaluated (Laibacher and Anjos, 2019). We used an M2u-Net (Laibacher, 2019), which was initialized using pre-trained VGG16 weights and then adapted to the segmentation of both vessels and the laser spot via 200 hand-labeled samples and a fixed number of training steps (F1 score 0.96/0.98 for vessel and laser segmentation, respectively, after training). Our reference implementation of this architecture has been previously published (Laibacher, n.d.). The architectural choice allows for both training and inference at original sample resolution (1040 × 1392 pixels). A separate set of 100 hand-labeled samples was used to fine-tune thresholding and to evaluate the final deep neural network performance (F1 score 0.87/0.78 for vessel/laser). The deep segmentation outputs binary masks with the same dimension as input images, indicating where both vessels and laser are located. We then evaluated the centroid of the laser reflection and proceeded to extract a topological skeleton of the vessel structure. Next, we determined the closest point C on the skeleton to the laser centroid. The width of the vessel was then measured around C, on the vessel binary mask, using an orthogonal direction to the vessel, estimated on the direction of the vessel skeleton around C.

Software 2 was evaluated to compare the performance with software 1 on a set of annotated images: 208 images were used to train the deep neural network model powering software 2 while 108 images were hold out for paired comparisons with software 1. Annotations (i.e. vessel delineations) were performed by two individuals (annotator 1 and 2) allowing us to also evaluate inter-observer agreement. The accuracy of software 1, software 2 and inter-observer agreement were evaluated by comparing the measured vessel widths for the vessel which was closest to the laser beam.

2.3.2. Spectra

To determine the cut-off frequency (f_c) of each spectrum, we used an automated spectra analysis, assuming a rectangular distribution. Assuming that the power spectrum is given by $\{S_i\}$ where i corresponds to a given frequency and goes from 1 to n. The ideal case (rectangular

distribution of the spectra) is given by: $\{S_k\} = X$ for $k \leq f_c$ and $\{S_k\} = Y$ for $k \geq f_c$ where $1 \leq k \leq n$, f_c defines the cut-off frequency and Y the noise of the system. The ratio X/Y gives the signal-to-noise ratio (SNR). For the automated spectra analysis (Petrig and Riva, 1988), the position f_c corresponds to the minimum of the residual:

$$r_k = \sum_{i=1}^{k} (S_i - X)^2 + \sum_{i=k}^{n} (S_i - Y)^2$$

Spectra are often a superposition of a signal from the vessel (step distribution) and from the tissue behind or near the vessel (decreasing distribution) depending on the exact position of the probing beam. To determine the cut-off frequency of a spectrum, we ran from the lower frequencies to the higher frequencies and stop when all further powers were lower than half of the current frequency, which was then considered the cut-off frequency. This algorithm excluded noisy spectrum automatically because we ran up to the digitalized maximum frequency (10 kHz).

2.4. Statistical analysis

All analyses were performed with R (*R Core Team (2018). R: A language and environment for statistical computing. R Foundation for Statistical Computing, Vienna, Austria. Url https://www.R-project.org/*, n.d.). Results are presented as the mean ± standard deviation (SD). The Pearson test was used to evaluate the correlation between total RBF and subject characteristics. Student's *t*-test was used to compare unpaired continuous variables with normal distribution, and the paired t-test was used to compare paired continuous variables with normal distribution.

3. Results

3.1. Subjects

Systemic and ocular characteristics of healthy subjects (n = 15) and patients with retinal vein occlusion (n = 6) are summarized in Table 1. Patients exhibited BRVO in one case, hemiCRVO in one case, and CRVO in four cases. The series of 6 patients described here came from a cohort of 16 included RVO patients. Indeed, data from 10 RVO patients were excluded due to major difficulties to obtain a good fixation and therefore reliable data from spectrum analysis. Only one case (with BRVO) was associated with retinal ischemia in the area of vein occlusion. The duration of symptoms before RBF measurement was 17 ± 10 days.

Table 1
Clinical characteristics of healthy subjects and patients with retinal vein occlusion (RVO).

	Healthy subjects (n = 15)	RVO patients (n = 6)
	Mean ± SD (range)	Mean ± SD (range)
Age, years	38.8 ± 17.7 (22–73)	68.6 ± 10.2 (52–78)
Sex, female/male	8/7	2/4
Body mass index	22.3 ± 2.8 (18.4–29.3)	21.7 ± 3.2 (18.7–27.7)
Systolic blood pressure, mmHg	122.4 ± 10.6 (104–142)	131 ± 14 (110–145)
Diastolic blood pressure, mmHg	75.6 ± 11.2 (56–93)	80 ± 10 (69–95)
Heart rate, bpm	73 ± 9.6 (55–93)	77 ± 14.3 (64–104)
Hematocrit, %	41.5 ± 3.4 (36–47)	41.0 ± 2.9 (36–45)
Eye included, right/left	3/12	1/5
Spherical equivalent, diopters	0 ± 1.3 (−2.75–2)	−0.8 ± 0.7 (−1.75–0.25)
Intraocular pressure, mmHg	14.4 ± 2.7 (9–20)	15.5 ± 3.8 (10–20)
Axial length, mm	23.5 ± 0.8 (22.3–24.8)	23.4 ± 0.5 (22.8–24.3)
Central subfield thickness, µm	265.8 ± 14.5 (232–288)	372 ± 163 (263–696)

bpm = beat per minute.

3.2. Measurements of retinal vessel diameters

Over the set of 108 annotated images, software 1 provided an output to 68 % of the images (73/108) whereas software 2 was successful in 100 % of the cases. We observed an average difference of 9 ± 10 pixels (10.3 ± 12.0 µm) comparing two different human observers which corresponds to 13 % difference in the estimation of the relative vessel width. Accordingly, both softwares 1 and 2 provided similar evaluation scores, with software 2 being able to analyze all images.

Based on a set of 73 images (Table 2), software 2 provided wider measurements of retinal vascular diameters (88.3 ± 16.9 µm) as compared with Software 1 (84.1 ± 17.6 µm, $p = 0.03$, paired comparisons). Values obtained using both softwares were well correlated ($r = 0.6$, $p < 0.001$). Variability of vascular diameter measurements of the 40 images in a single recording was higher using Software 2 (SD = 6.8 ± 4.6 pixels) as compared with Software 1 (SD = 2.9 ± 2.5 pixels, $p < 0.001$).

In the 15 healthy subjects, 308 RBF measurements were performed, including 12,320 AO images. Software 1 provided diameter measurements in 7998 images (64.9 %).

3.3. Retinal blood flow in healthy subjects

The total RBF was obtained from retinal veins in 15 healthy subjects. The characteristics of healthy subjects are listed in Table 1. Total RBF was 37.84 ± 6.81 µl/min. Fig. 1 illustrates RBF measurements in one healthy subject allowing for the calculation of total RBF.

All RBF measurements in healthy subjects are summarized in Fig. 2A and B. There was a significant linear correlation between retinal vessel diameter and maximal velocity (slope = 0.1016; $p < 0.001$; $r^2 = 0.8597$; Fig. 2A) and a significant power curve correlation between retinal vessel diameter and blood flow ($3.63 \times 10^{-5} \times D^{2.54}$; $p < 0.001$; $r^2 = 0.7287$; Fig. 2B).

Eight venous bifurcations in eight healthy subjects were analyzed from the measurements of a proximal vessel and the two distal vessels (Table 3). The comparison between proximal vessel flow and the sum of the two distal vessel flows shows a mean difference of 11.9 ± 4.3 % (range: 6–17.3 %).

3.4. Retinal blood flow in retinal vein occlusion

Characteristics of OVR patients are listed in Table 1. Three patients

Table 2
Evaluation of softwares 1 and 2 on 108 annotated images.

Model	Successful samples	Vessel width	Absolute vessel width difference versus Annotator 1	Vessel width (on 73 paired samples with software 1)	Absolute vessel width difference versus Annotator 1 (on 73 paired samples with software 1)
Annotator 2	108/108 (100 %)	86.3 ± 19.1 µm	10.3 ± 12.0 µm	86.9 ± 18.7 µm	9.4 ± 8.4 µm
Software 1	73/108 (68 %)	84.1 ± 17.6 µm	10.3 ± 10.3 µm	84.1 ± 17.6 µm	10.3 ± 10.3 µm
Software 2	108/108 (100 %)	87.5 ± 20.3 µm	11.4 ± 11.7 µm	88.3 ± 16.9 µm	9.7 ± 7.6 µm

Annotators 1 and 2 (TM, AA) delineated the borders of vessels present on the images as well as the location of the laser beam. Software 2 provided wider measurements of retinal vascular diameters as compared with Software 1 ($p = 0.03$, paired comparisons). Average values and standard deviations are given in micrometers (µm). The relationship between pixels and distance is 1 pixel = 1.14. micrometers (µm).

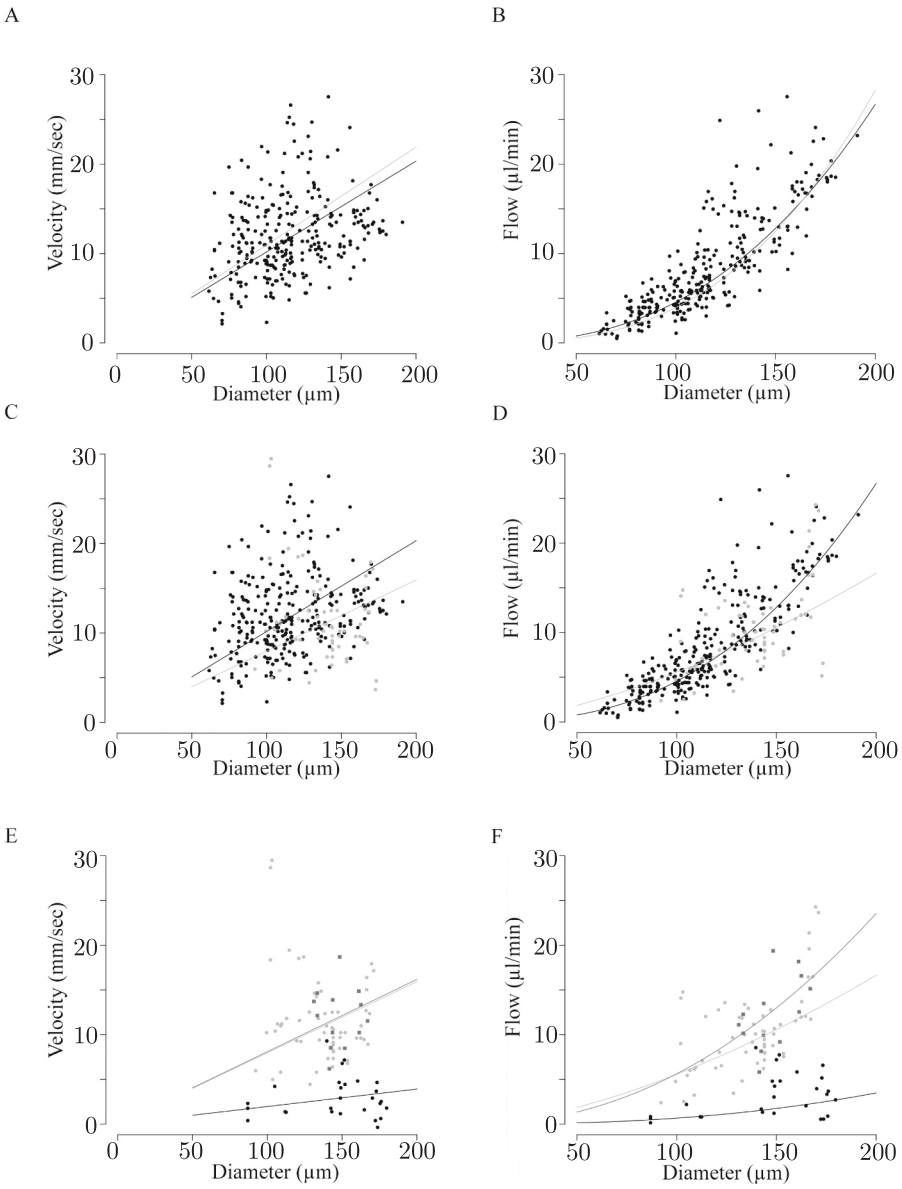

Fig. 2. Correlation between retinal vein diameter, velocity and flow in healthy subjects and patients with retinal vein occlusion.
(A) For healthy subjects, the relationship between velocity and diameter is linear (slope = 0.1016; $p < 0.001$; $r^2 = 0.8597$, black line), which is consistent with the princeps publication by Riva et al. (Riva et al., 1985) (slope = 0.1094, gray line).
(B) For healthy subjects, the relationship between flow and diameter exhibits a power curve according to the formula $Q = 3.63 \times 10^{-5} \times D^{2.54}$ ($p < 0.001$; $r^2 = 0.7287$, black line), which is consistent with the previous publication of Riva et al. (Riva et al., 1985; Riva et al., n.d.) ($Q = 8.25 \times 10^{-6} \times D^{2.84}$, gray line).
(C & D) In the same way as (A) and (B), this plot represents the relation of velocity or flow to diameter, but it compares the measurements performed on vessels in healthy (black) and non-occluded vessels in RVO patients (gray). For non-occluded vessels in RVO patients, the slope between diameter and velocity was 0.0796 ($p < 0.001$; $r^2 = 0.7934$) and the relation between diameter and flow was $Q = 3.82 \times 10^{-3} \times D^{1.58}$ ($p < 0.001$; $r^2 = 0.2772$).
(E & F) This plot represents the relation of velocity of flow to diameter for measurements performed on vessels in different RVO patients: non-occluded vessels (gray circle), occluded vessels (black circles), and occluded vessels 1 month after one aflibercept injection (gray cubes). For occluded vessels, the slope between diameter and velocity was 0.0195 ($p < 0.001$; $r^2 = 0.6068$) and the relation between diameter and flow was $Q = 9.91 \times 10^{-6} \times D^{2.41}$ ($p < 0.01$; $r^2 = 0.2526$). For occluded vessels 1 month after treatment, the slope was 0.081 ($p < 0.001$; $r^2 = 0.9223$) and the relation between diameter and flow was $Q = 4.08 \times 10^{-4} \times D^{2.06}$ ($p < 0.08$; $r^2 = 0.1782$).

had branch RVO (BRVO; Fig. 3A), while three patients suffered from central RVO (CRVO; Fig. 3B). Two patients underwent treatment with intravitreal injection of aflibercept (Fig. 3C). The median delay between the onset of symptoms and the flow measurement procedure was 19 days (10.2–24.7). In all cases, RBF had decreased in occluded veins, despite a wider diameter of retinal veins, as can be seen on the spectrum analysis (Fig. 3). We noted a relationship in non-occluded vessels between vessel diameter and maximal velocity (slope = 0.0796; $p < 0.001$; $r^2 = 0.7934$) or RBF ($Q = 3.82 \times 10^{-3} \times D^{1.58}$; $p < 0.001$; $r^2 = 0.2772$) similar to that described in healthy subjects (Fig. 2C and D).

The comparison between the occluded vessels (3.51 ± 2.25 µl/min) and similar vessels in the contralateral eye (11.07 ± 4.53 µl/min) showed a significant decrease in RBF ($p < 0.001$). For occluded vessels, the slope between diameter and velocity was 0.0195 ($p < 0.001$; $r^2 = 0.6068$) and the relation between diameter and flow was $Q = 9.91 \times 10^{-6} \times D^{2.41}$ ($p < 0.01$; $r^2 = 0.2526$). RBF in the inferior occluded vein of the eye with ischemic BRVO was 0.5 µl/min (n = 1) whereas mean RBF occluded veins from eyes with non-ischemic forms (n = 5 CRVOs) was

Table 3
Retinal blood flow in vessel bifurcations.

Vessel $_{Branch\ 1}$		Vessel $_{Branch\ 2}$		$V_{B1} + V_{B2}$	Vessel $_{Parent}$		Δ/V_P
86 µm	2.06 µl/min	156 µm	11.29 µl/min	13.35 µl/min	169 µm	17.32 µl/min	12.3 %
125 µm	5.06 µl/min	105 µm	3.5 µl/ min	8.56 µl/ min	132 µm	7.13 µl/ min	7.5 %
134 µm	9.82 µl/min	109 µm	8.53 µl/ min	18.35 µl/min	158 µm	16.86 µl/min	17.3 %
131 µm	9.89 µl/min	112 µm	5.53 µl/ min	15.42 µl/min	159 mm	13.46 µl/min	14.4 %
116 µm	6.84 µl/min	82 µm	1.58 µl/ min	8.42 µl/ min	126 µm	8.57 µl/ min	7.4 %
81 µm	4.57 µl/min	65 µm	2.51 µl/ min	7.08 µl/ min	89 µm	6.72 µl/ min	6.0 %
129 µm	9.53 µl/min	78 µm	4.99 µl/ min	14.53 µl/min	165 µm	17.51 µl/min	13.5 %
98 µm	8.92 µl/min	109 µm	8.59 µl/ min	17.51 µl/min	155 µm	16.35 µl/min	16.5 %

3.79 ± 1.57 µl/min.

For the CRVO patient who underwent aflibercept treatment, we then observed an at least partial recovery of flow, as well as an improvement in visual acuity and the macular edema (Fig. 3C). For occluded vessels 1 month after intravitreal treatment, the slope was 0.081 ($p < 0.001$; $r^2 = 0.9223$) and the relation between diameter and flow was $Q = 4.08 \times 10^{-4} \times D^{2.06}$ ($p < 0.08$; $r^2 = 0.1782$). Fig. 2E and F summarize the measurements performed in non-occluded veins, occluded veins at diagnosis, and occluded veins after aflibercept injection.

4. Discussion

Our study of the new AO-LDV prototype showed: (1) the feasibility of RBF measurements in healthy subjects and RVO patients, (2) measurements of RBF are in the range of published data using LDF technology, (3) measurements of vein diameters can be automatically computed using appropriate new software, (4) RBF after retinal vein occlusion is significantly lowered and the relationship between retinal vein diameter and flow is modified when compared to normal eyes.

In previous studies, the authors independently measured red blood cell velocity and vascular diameter at two different times, which represents a technical and scientific limitation. The AO-LDV prototype allows for the simultaneous acquisition of diameters and velocities and thus the calculation of RBF. The use of a laser during the acquisition of AO images does not allow for use of the averaged image acquired during a 4-s recording and processed with the rtX1 software. For this reason, retinal vascular diameter was calculated from between one and several raw images acquired during the 4-s recording. Accordingly, the resolution of raw images was 1392 × 1040 px instead of 1500 × 1770 for averaged images.

Automated calculation of vascular diameters was performed using dedicated software. Software 1 was used as the standard reference and the diameter was obtained for 64.9 % of images. To facilitate automatic measurement of retinal diameters and to improve selection and identification of the retinal vessel, we also evaluated an innovative approach involving deep neural networks (software 2). Data obtained from each 4-s recording using softwares 1 and 2 were well correlated, and paired comparison showed a significant difference between both implementations of 3.7 µm, which is in the range of variability of both applications.

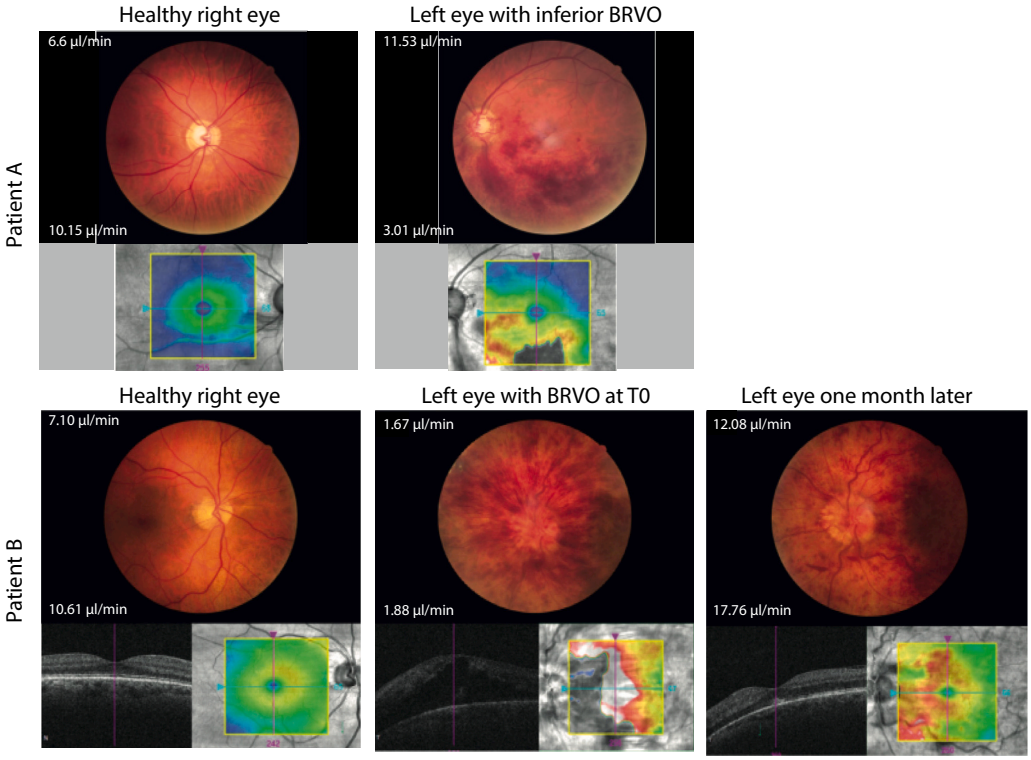

Fig. 3. Retinal blood flow in eyes with retinal vein occlusion.
Fundus photography, optical coherence tomography, and RBF measurement for a number of RVO patients. Measurements of RBF in superior and inferior temporal veins are recorded in the figs.
1- RBF was measured in temporal veins in a patient in the right healthy eye (1A) and the left eye with inferior CRVO (1B). The RBF of the occluded vein was significantly decreased when compared with the contralateral inferior temporal vein.
2- RBF was measured in temporal veins of the right healthy eye (2A) and the inferior left eye with CRVO (2B, T0). The RBF in the left eye, both in the inferior and superior temporal veins, was decreased compared with the contralateral eye. Measurements of RBF at 1 month after the first injection of aflibercept (2C) showed a significant increase in RBF in the temporal occluded veins.

As stated in the methods, softwares 1 and 2 were only evaluated on a set of 108 annotated images. A preliminary test shows that software 2 is able to provide a vascular diameter in 99.5 % of 12,320 images from 308 RBF measurements. This exploratory study showed that the mean difference between softwares was tiny, about 3,7 μm, i.e. 5 %. Further studies are necessary to compare softwares 1 and 2 on a larger set of uniformly sampled annotated images, i.e. images that encompass enough statistical variability.

For the spectrum analysis, the automatic analysis described in the method section was not always effective for the cut-off determination depending on the quality of the spectrum. For this reason, a "human" selection of spectra was used to identify spectra with a high level of noise and to select spectra. One perspective would be the development of a software that excludes low-quality spectra associated with the parallax phenomenon.

The rtx1 optical system has two optical paths, one for illumination and one for AO imaging. Due to the restricted space and choice of wavelength, the Doppler system was introduced in the illumination path, which does not correct for the eye aberration and corrects only partially for the dioptric error of the eye. If the focal plane of the Doppler system does not match the retinal plane, then parallax occurs and the light detected does not match that of the vessel. For this reason, we added an extra step to set the focal plane of the Doppler system on the retinal plane. This was done by replacing detection by laser sources and moving theses sources onto the probing beam. However, this technique as used in the present study is time-consuming (i.e., 40 min for measuring all major retinal veins in one eye). We acknowledge that this AOLDV device was not directly compared to other devices such as Canon LDV or laser speckle flowgraphy, which would be a further study. Previous experiments validated our experimental device with in vitro measurements (Truffer et al., 2020).

Previous studies using different technologies reported the total RBF in humans based on vein measurements (Table 4). In our study, the total RBF varies between 23.83 and 50.7 μl/min, which is consistent with previous studies. With a device based on the same fundamental principle, bidirectional LDV and monochromatic fundus photographs, Riva et al. found a total RBF that varies between 23.8 and 40.9 μl/min (Riva et al., 1985), Grunwald et al. between 25.9 and 44.4 μl/min (Grunwald et al., 1992), and Garhofer et al. between 23.0 and 80.8 μl/min (Garhofer et al., 2012). AO-LDV measurements also showed a similar relationship between retinal vein diameter and velocity to that of the previous study by Rival C et al. (Riva et al., 1985). We also showed a slight correlation between total RBF and OPP, consistent with a previous study by Garhofer (Garhofer et al., 2012). This is probably due to an autoregulation of RBF and the low range of OPP in our healthy subjects (between 40 and 70 mmHg) (Pournaras et al., 2008).

The difference in RBF observed when studying vessel bifurcations underlines the variability of velocity measurements rather than measurements of vein diameters using our prototype. A reproducibility test was done on five vessels of one eye with three measurements per vessel. We showed that the variability of vessel velocity (mean coefficient of variation of 9.38) was higher than the variability of vessel diameter (mean coefficient of variation of 2.89).

Table 4
Review of the literature for the measurement of total retinal venous flow in healthy subjects. TRBF: total retinal blood flow, LDV: laser Doppler velocimetry, FD-OCT: Fourier-domain optical coherence tomography.

Study	Measurement technique	No. of subjects	Age (years, range)	TRBF (μl/min, range)
Our study	AO-LDV	15	39 (22–73)	23.83–50.7
(Riva et al., 1985)	LDV	7	34 (20–45)	23.8–40.9
(Grunwald et al., 1992)	LDV	12	32 (19–45)	25.9–44.4
(Doblhoff-Dier et al., 2014)	FD-OCT	4	Unknown	32.5–42.4
(Garhofer et al., 2012)	LDV	64	32 (18–45)	23.3–80.8

Our results show significantly reduced RBF in occluded veins, in contrast to that reported by Kohner et al. (Chen et al., 1998) using bidirectional LDV. Our conclusions are limited by the limited number of patients included according to a strict selection criterion (absence of anti-hypertensive treatment). In RVO, we found lower RBF (3.51 ± 2.25 μl/min) at baseline in occluded vessels than that described by Kohner (13.7 ± 5.8 μl/min) whereas RBF values in healthy vessels were similar (11.07 ± 4.53 μl/min vs 14.2 ± 4.1 μl/min). Another study that reported RBF using laser speckle flowgraphy showed that RBF in occluded vessels (BRVO) was reduced by 20 % as compared with contralateral retinal veins of the same eye (Noma et al., 2016). This reduction was estimated to be 68 % in our series, when we compared occluded vessels with healthy vessels in the contralateral eye. Our data also may suggest that RBF is reduced in ischemic RVO as compared with non-ischemic RVO. However, this result should be confirmed among a larger series. The measurement of RBF will offer the ability to evaluate future treatment for improving blood flow.

Riva and coll. (Logean et al., 2003) has demonstrated that the retinal flow in vessels of healthy, young subjects is laminar. According to the Poisseuille's equation, this type of flow is proportional to the fourth power of the diameter (i.e. R^4). We found a power factor of 2.54 in healthy eyes which is close to the 2.84 factor reported by Riva (Riva et al., 1985) using LDV and lower than that found by Garcia (Garcia et al., 2002), a factor of 3.5 using Canon LDV. For subjects with RVO, the calculation gave the lower factor of 1.58 in non-occluded vessels and 2.41 in occluded vessels, which suggests that other physical quantities than perfusion pressure and blood vessel length are involved.

The increase of RBF after anti-VEGF treatment (about +30 %) has been previously described using laser speckle flowgraphy technique in non-ischemic eyes (Matsumoto et al., 2021). In one case of CRVO, we illustrated a significant increase in RBF at one month after anti-VEGF treatment. The mechanism by which the effect of anti-VEGF could be driven is not known since anti-VEGF drugs may induce decrease (Fukami et al., 2017; Sacu et al., 2011), no change (Bek et al., 2008; Nagaoka et al., 2014) or increase (Micieli et al., 2012; Noma et al., 2016) in retinal vein diameter. The effect of anti-VEGF drugs is complex, associated with the intraocular level of VEGF (Nagaoka et al., 2014; Yamada et al., 2015) and also to the extent of vein occlusion and/or associated ischemia.

We acknowledge several technical limitations relative to this AOLDV device: (1) there is no eye-tracking and therefore the fixation of the subject should be excellent in order to keep the laser beam on the center of retinal vessels. This may explain why several spectra from LDV measurement should be excluded for final analysis. Moreover, this limits the use of this system to subjects with a good fixation, and therefore limits the routine use of this device in ophthalmology (2) One should also note that software 1 used for evaluation of RBF provided an output in about 65 % of the cases, due to the following reasons: (1) the subject was blinking with no apparent vessels, (2) the AO illumination failed to correctly illuminate the field-of-view and (3) in case many vessels were in the area of the laser beam, software 1 poorly detected the edges of the vessel of interest. Finally, since our AO-LDV acquires retinal vessel diameter measurements every 100 msecondes during 4 secondes, the overall measurement considers measurements during diastole and systole. Pulsatility per se is not therefore considered in the analysis. The cardiac cycle mainly influences blood flow velocity profiles in retinal arteries and in a lesser extent in veins (Knudtson, 2004; Riva et al., 1985; Zhong et al., 2011), we focused our measurement on retinal veins and acknowledge that some minor variability of RBF measurement in relationship with pulsatility could be encountered. As noticed previously, the major limitation of the technique is the need of an excellent macular fixation, even in the controlateral healthy eye, especially in aged patients.

In conclusion these new developments using AO-LDV are encouraging for the non-invasive evaluation of RBF in humans and offer new opportunity to study RBF in patients with retinal vascular disease. This study should prompt future technical improvement, including the use of the optical path of rtX1 for the LDV part of the system, to overcome the parallax problem and improve the quality of the spectra acquired.

CRediT authorship contribution statement

Thibaud Mautuit: Conceptualization, Data curation, Formal analysis, Investigation, Writing – original draft, Writing – review & editing. **Pierre Cunnac:** Data curation, Formal analysis, Investigation, Writing – original draft. **Frédéric Truffer:** Conceptualization, Data curation, Methodology, Software, Writing – original draft. **André Anjos:** Software, Writing – original draft, Writing – review & editing. **Rebecca Dufrane:** Data curation, Writing – original draft. **Gilbert Maître:** Software, Writing – original draft, Writing – review & editing. **Martial Geiser:** Conceptualization, Funding acquisition, Methodology, Project administration, Software, Supervision, Writing – original draft, Writing – review & editing. **Christophe Chiquet:** Conceptualization, Data curation, Formal analysis, Funding acquisition, Investigation, Methodology, Project administration, Resources, Writing – original draft, Writing – review & editing.

Declaration of competing interest

The authors declare that they have no known competing financial interests or personal relationships that could have appeared to influence the work reported in this paper.

Data availability

Data will be made available on request.

Acknowledgments

We would like to thank Sebastien Bailly (HP2 Laboratory, INSERM U1042, Grenoble, France) for assistance with the statistical analysis. The study was funded by the Association for Research and Education in Ophthalmology (ARFO, Grenoble, France), the French Ministry of Foreign affairs of France and Switzerland (Germaine de Stael grant), University hospital of Grenoble-Alpes (DRCI grant, Grenoble, France), HES-SO (Sion, Switzerland), and Bayer Healthcare SAS.

Appendix A. Supplementary data

Supplementary data to this article can be found online at https://doi.org/10.1016/j.mvr.2023.104648.

References

Arsene, S., Giraudeau, B., Le Lez, M.-L., Pisella, P.J., Pourcelot, L., Tranquart, F., 2002. Follow up by colour Doppler imaging of 102 patients with retinal vein occlusion over 1 year. Br. J. Ophthalmol. 86, 1243–1247. https://doi.org/10.1136/bjo.86.11.1243.

Bek, T., Hajari, J., Jeppesen, P., 2008. Interaction between flicker-induced vasodilatation and pressure autoregulation in early retinopathy of type 2 diabetes. Graefes Arch. Clin. Exp. Ophthalmol. Albrecht Von Graefes Arch. Klin. Exp. Ophthalmol. 246, 763–769. https://doi.org/10.1007/s00417-008-0766-y.

Bennett, A.G., Rudnicka, A.R., Edgar, D.F., 1994. Improvements on Littmann's method of determining the size of retinal features by fundus photography. Graefes Arch. Clin. Exp. Ophthalmol. Albrecht Von Graefes Arch. Für Klin. Exp. Ophthalmol. 232, 361–367.

Burgansky-Eliash, Z., Barash, H., Nelson, D., Grinvald, A., Sorkin, A., Loewenstein, A., Barak, A., 2014. Retinal blood flow velocity in patients with age-related macular degeneration. Curr. Eye Res. 39, 304–311. https://doi.org/10.3109/02713683.2013.840384.

Chen, H.C., Gupta, A., Wiek, J., Kohner, E.M., 1998. Retinal blood flow in nonischemic central retinal vein occlusion. Ophthalmology 105, 772–775. https://doi.org/10.1016/S0161-6420(98)95013-8.

Doblhoff-Dier, V., Schmetterer, L., Vilser, W., Garhöfer, G., Gröschl, M., Leitgeb, R.A., Werkmeister, R.M., 2014. Measurement of the total retinal blood flow using dual beam Fourier-domain Doppler optical coherence tomography with orthogonal detection planes. Biomed. Opt. Express 5, 630–642. https://doi.org/10.1364/BOE.5.000630.

Ehrlich, R., Kheradiya, N.S., Winston, D.M., Moore, D.B., Wirostko, B., Harris, A., 2009. Age-related ocular vascular changes. Graefes Arch. Clin. Exp. Ophthalmol. 247, 583–591. https://doi.org/10.1007/s00417-008-1018-x.

Fukami, M., Iwase, T., Yamamoto, K., Kaneko, H., Yasuda, S., Terasaki, H., 2017. Changes in retinal microcirculation after intravitreal ranibizumab injection in eyes with macular edema secondary to branch retinal vein occlusion. Invest. Ophthalmol. Vis. Sci. 58, 1246–1255. https://doi.org/10.1167/iovs.16-21115.

Garcia, J.P.S., Garcia, P.T., Rosen, R.B., 2002. Retinal blood flow in the normal human eye using the canon laser blood flowmeter. Ophthalmic Res. 34, 295–299. https://doi.org/10.1159/000065600.

Garhofer, G., Werkmeister, R., Dragostinoff, N., Schmetterer, L., 2012. Retinal blood flow in healthy young subjects. Invest. Ophthalmol. Vis. Sci. 53, 698–703. https://doi.org/10.1167/iovs.11-8624.

Grunwald, J.E., Riva, C.E., Baine, J., Brucker, A.J., 1992. Total retinal volumetric blood flow rate in diabetic patients with poor glycemic control. Invest. Ophthalmol. Vis. Sci. 33, 356–363.

Guan, K., Hudson, C., Flanagan, J.G., 2003. Variability and repeatability of retinal blood flow measurements using the Canon Laser Blood Flowmeter. Microvasc. Res. 65, 145–151. https://doi.org/10.1016/s0026-2862(03)00007-4.

Gutfreund, S., Izkhakov, E., Pokroy, R., Yaron, M., Yeshua, H., Burgansky-Eliash, Z., Barak, A., Rubinstein, A., 2013. Retinal blood flow velocity in metabolic syndrome. Graefes Arch. Clin. Exp. Ophthalmol. 251, 1507–1513. https://doi.org/10.1007/s00417-013-2325-4.

Knudtson, M.D., 2004. Variation associated with measurement of retinal vessel diameters at different points in the pulse cycle. Br. J. Ophthalmol. 88, 57–61. https://doi.org/10.1136/bjo.88.1.57.

Koch, E., Rosenbaum, D., Brolly, A., Sahel, J.-A., Chaumet-Riffaud, P., Girerd, X., Rossant, F., Paques, M., 2014. Morphometric analysis of small arteries in the human retina using adaptive optics imaging: relationship with blood pressure and focal vascular changes. J. Hypertens. 32, 890–898. https://doi.org/10.1097/HJH.0000000000000095.

Laibacher, T., 2019. M 2 U-Net: effective and efficient retinal vessel segmentation for real-world applications [WWW document]. URL. https://www.semanticscholar.org/paper/M-2-U-Net-%3A-Effective-and-Efficient-Retinal-Vessel-Laibacher/af74acfbc9c55f72c42cf18b98a204b2508e096b. (Accessed 28 October 2021).

Laibacher, T., n.d. https://gitlab.idiap.ch/bob/bob.ip.binseg.

Laibacher, T., Anjos, A., 2019. On the Evaluation and Real-World Usage Scenarios of Deep Vessel Segmentation for Funduscopy. ArXiv190903856 Cs.

Leitgeb, R.A., Werkmeister, R.M., Blatter, C., Schmetterer, L., 2014. Doppler optical coherence tomography. Prog. Retin. Eye Res. 41, 26–43. https://doi.org/10.1016/j.preteyeres.2014.03.004.

Lim, M., Sasongko, M.B., Ikram, M.K., Lamoureux, E., Wang, J.J., Wong, T.Y., Cheung, C. Y., 2013. Systemic associations of dynamic retinal vessel analysis: a review of current literature. Microcirculation 20, 257–268. https://doi.org/10.1111/micc.12026.

Logean, E., Schmetterer, L., Riva, C., 2003. Velocity profile of red blood cells in human retinal vessels using confocal scanning laser Doppler velocimetry. Laser Phys. 13, 45–51.

Matsumoto, M., Suzuma, K., Akiyama, F., Yamada, K., Harada, S., Tsuiki, E., Kitaoka, T., 2021. Retinal vascular resistance significantly correlates with visual acuity after 1 year of anti-VEGF therapy in central retinal vein occlusion. Transl. Vis. Sci. Technol. 10, 19. https://doi.org/10.1167/tvst.10.11.19.

Micieli, J.A., Tsui, E., Lam, W.-C., Brent, M.H., Devenyi, R.G., Hudson, C., 2012. Retinal blood flow in response to an intravitreal injection of ranibizumab for neovascular age-related macular degeneration. Acta Ophthalmol. 90, e13–e20. https://doi.org/10.1111/j.1755-3768.2011.02209.x.

Nagaoka, T., Sogawa, K., Yoshida, A., 2014. Changes in retinal blood flow in patients with macular edema secondary to branch retinal vein occlusion before and after intravitreal injection of bevacizumab. Retina Phila. Pa 34, 2037–2043. https://doi.org/10.1097/IAE.0000000000000172.

Noma, H., Yasuda, K., Minezaki, T., Watarai, S., Shimura, M., 2016. Changes of retinal flow volume after intravitreal injection of bevacizumab in branch retinal vein occlusion with macular edema: a case series. BMC Ophthalmol. 16 https://doi.org/10.1186/s12886-016-0239-8.

Pemp, B., Schmetterer, L., 2008. Ocular blood flow in diabetes and age-related macular degeneration. Can. J. Ophthalmol. 43, 295–301. https://doi.org/10.3129/i08-049.

Pemp, B., Polska, E., Karl, K., Lasta, M., Minichmayr, A., Garhofer, G., Wolzt, M., Schmetterer, L., 2010. Effects of antioxidants (AREDS medication) on ocular blood flow and endothelial function in an endotoxin-induced model of oxidative stress in humans. Invest. Ophthalmol. Vis. Sci. 51, 2–6. https://doi.org/10.1167/iovs.09-3888.

Petrig, B.L., Riva, C.E., 1988. Retinal laser Doppler velocimetry: toward its computer-assisted clinical use. Appl. Opt. 27, 1126–1134. https://doi.org/10.1364/AO.27.001126.

Pournaras, C.J., Riva, C.E., 2013. Retinal blood flow evaluation. Ophthalmologica 229, 61–74. https://doi.org/10.1159/000338186.

Pournaras, C.J., Rungger-Brändle, E., Riva, C.E., Hardarson, S.H., Stefansson, E., 2008. Regulation of retinal blood flow in health and disease. Prog. Retin. Eye Res. 27, 284–330. https://doi.org/10.1016/j.preteyeres.2008.02.002.

Puyo, L., Paques, M., Atlan, M., 2020. Spatio-temporal filtering in laser Doppler holography for retinal blood flow imaging. Biomed. Opt. Express 11, 3274–3287. https://doi.org/10.1364/BOE.392699.

R Core Team (2018). R: a language and environment for statistical computing. R Foundation for Statistical Computing, Vienna, Austria. URL https://www.R-project.org/, n.d.

Rechtman, E., Harris, A., Kumar, R., Cantor, L.B., Ventrapragada, S., Desai, M., Friedman, S., Kagemann, L., Garzozi, H.J., 2003. An update on retinal circulation assessment technologies. Curr. Eye Res. 27, 329–343. https://doi.org/10.1076/ceyr.27.6.329.18193.

Ritt, M., Harazny, J.M., Ott, C., Raff, U., Bauernschubert, P., Lehmann, M., Michelson, G., Schmieder, R.E., 2012. Impaired increase of retinal capillary blood flow to flicker light exposure in arterial hypertension. Hypertension 60, 871–876. https://doi.org/10.1161/HYPERTENSIONAHA.112.192666.

Riva, C., Ross, B., Benedek, G.B., 1972. Laser Doppler measurements of blood flow in capillary tubes and retinal arteries. Investig. Ophthalmol. 11, 936–944.

Riva, C.E., Grunwald, J.E., Sinclair, S.H., Petrig, B.L., 1985. Blood velocity and volumetric flow rate in human retinal vessels. Invest. Ophthalmol. Vis. Sci. 26, 1124–1132.

Riva, C.E., Grunwald, J.E., Sinclair, S.H., Perrig, B.L., n.d. Blood Velocity ond Volumetric Flow Rate in Human Retinal Vessels vol. 26, 9.

Sacu, S., Pemp, B., Weigert, G., Matt, G., Garhofer, G., Pruente, C., Schmetterer, L., Schmidt-Erfurth, U., 2011. Response of retinal vessels and retrobulbar hemodynamics to intravitreal anti-VEGF treatment in eyes with branch retinal vein occlusion. Invest. Ophthalmol. Vis. Sci. 52, 3046–3050. https://doi.org/10.1167/iovs.10-5842.

Sehi, M., Goharian, I., Konduru, R., Tan, O., Srinivas, S., Sadda, S.R., Francis, B.A., Huang, D., Greenfield, D.S., 2014. Retinal blood flow in glaucomatous eyes with single-Hemifield damage. Ophthalmology 121, 750–758. https://doi.org/10.1016/j.ophtha.2013.10.022.

Tranquart, F., Arsene, S., Aubert-Urena, A.S., Desbois, I., Audrerie, C., Rossazza, C., Pourcelot, L., 1998. Doppler assessment of hemodynamic changes after hemodilution in retinal vein occlusion. J. Clin. Ultrasound 26, 119–124. https://doi.org/10.1002/(SICI)1097-0096(199803/04)26:3<119::AID-JCU2>3.0.CO;2-P.

Truffer, F., Geiser, M., Chappelet, M.-A., Strese, H., Maître, G., Amoos, S., Aptel, F., Chiquet, C., 2020. Absolute retinal blood flowmeter using a laser Doppler velocimeter combined with adaptive optics. J. Biomed. Opt. 25 https://doi.org/10.1117/1.JBO.25.11.115002.

Werkmeister, R.M., Dragostinoff, N., Palkovits, S., Told, R., Boltz, A., Leitgeb, R.A., Gröschl, M., Garhöfer, G., Schmetterer, L., 2012. Measurement of absolute blood flow velocity and blood flow in the human retina by dual-beam bidirectional Doppler fourier-domain optical coherence tomography. Invest. Ophthalmol. Vis. Sci. 53, 6062–6071. https://doi.org/10.1167/iovs.12-9514.

Yamada, Y., Suzuma, K., Matsumoto, M., Tsuiki, E., Fujikawa, A., Harada, T., Kitaoka, T., 2015. Retinal blood flow correlates to aqueous vascular endothelial growth factor in central retinal vein occlusion. Retina Phila. Pa 35, 2037–2042. https://doi.org/10.1097/IAE.0000000000000595.

Yoshida, A., Feke, G.T., Mori, F., Nagaoka, T., Fujio, N., Ogasawara, H., Konno, S., Mcmeel, J.W., 2003. Reproducibility and clinical application of a newly developed stabilized retinal laser Doppler instrument. Am J. Ophthalmol. 135, 6.

Zhong, Z., Song, H., Chui, T.Y.P., Petrig, B.L., Burns, S.A., 2011. Noninvasive measurements and analysis of blood velocity profiles in human retinal vessels. Invest. Ophthalmol. Vis. Sci. 52, 4151–4157. https://doi.org/10.1167/iovs.10-6940.